

Flow development in a porous channel and tube

J. F. Brady

Department of Chemical Engineering, Massachusetts Institute of Technology, Cambridge, Massachusetts 02139

(Received 31 May 1983; accepted 4 November 1983)

The spatial development of the inlet velocity profile in a uniformly porous channel and tube is investigated. For tubes which are very long compared with their radius, it is shown that above a critical Reynolds number of 2.3 the inlet velocity profile does not necessarily decay into the fully developed, similarity profile for an infinite tube. Rather, the structure of the flow throughout the entire tube is influenced by the inlet profile. This loss of validity of the similarity solution is due to the fact that the tube is of finite length and the inlet profile is not of the similarity form. The actual length of the tube is, however, unimportant. Analogous results hold for the flow in a porous channel, with a critical Reynolds number of approximately 6.

I. INTRODUCTION

The flow in a porous channel or tube is one example of the broad class of flows caused or influenced by porous boundaries. These flows find application in a variety of physical situations such as the control of boundary-layer separation with suction or injection, filtration, membrane separation processes, and biological transport in living systems. Porous channel and tube flow are also of fundamental fluid mechanical interest because there exist exact similarity solutions to the Navier-Stokes equations for these problems; thus allowing, at least in principle, a comparison between an exact solution and an observable flow. It will be seen in this paper that this comparison is far from straightforward.

Berman¹ was the first to show that for a uniformly porous channel of semiinfinite extent there exists an exact solution to the Navier-Stokes equations of the form $u = -xf'(y)$, $v = f(y)$, and $p = p_0(y) + \frac{1}{2}\beta x^2$, where u and v are the x and y components of the fluid velocity, p is the pressure, and β is a constant (cf. Fig. 1). The similarity function f depends on a single parameter, the Reynolds number, $R = \rho Vh/\mu$, where V is the normal velocity through the channel walls [$V(R)$ positive corresponds to suction, negative to injection], h the channel half-width, ρ the fluid density, and μ its viscosity. The usual boundary conditions apply at

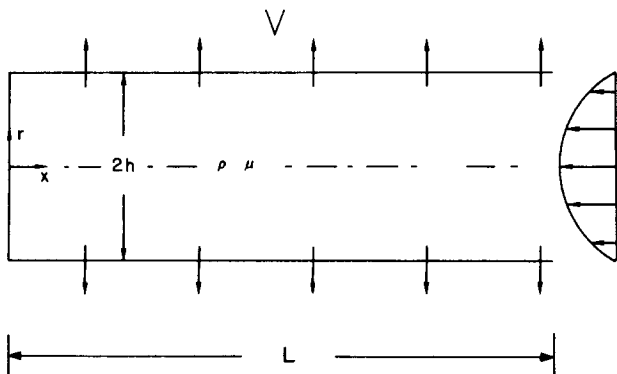


FIG. 1. Schematic diagram for the flow in a long, uniformly porous tube.

the channel wall; $u = 0$, $v = V$, and only symmetric flows— $\partial u/\partial y = v = 0$ at the channel centerline—are considered. An analogous similarity transformation holds for the flow in a porous tube, replacing $f'(y)$ by $f'(r)/r$ and $f(y)$ by $f(r)/r$ and h is now the tube radius. The similarity solutions have been thoroughly investigated by several authors, most notably Terrill.²⁻⁶

Briefly, the general features of these similarity solutions are as follows: For the two-dimensional porous channel flow there is a single continuous solution branch extending from $-\infty$ to $+\infty$ in R , and there are two additional solution branches appearing at $R = 12.165$ and extending to $+\infty$. These second solutions have rather unusual velocity profiles in which the minimum in the x component of velocity does not lie on the centerline. For the axisymmetric flow in a porous tube, there is also only a single solution for $R < 0$ (injection), which connects with a suction solution at $R \equiv 0$.⁷ For $R > 0$ the solution structure, being much more complex, is illustrated in Fig. 2, where the pressure coefficient β divided-

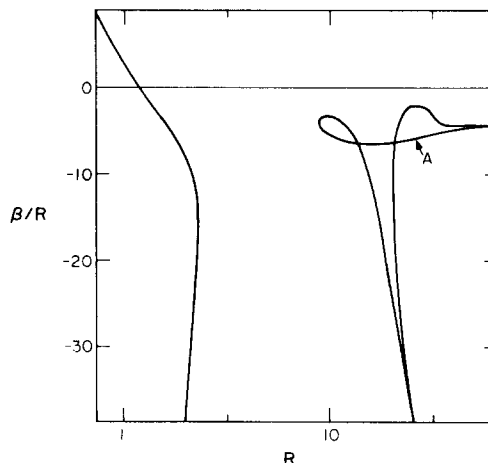


FIG. 2. The pressure coefficient β divided by the Reynolds number R of the similarity solutions for the axisymmetric flow in a uniformly porous tube. There is no solution in the Reynolds number range, $2.3 < R < 9.1$. The solution branch labeled A corresponds to the similarity solutions used in Fig. 5.

ed by R is plotted versus the Reynolds number. There are two solutions for $0 < R \leq 2.3$; the $\beta/R > 0$ branch connecting with the $R < 0$ solution. Then there is a gap in Reynolds number, $2.3 < R < 9.1$, within which there is no solution, and then multiple solutions appear for $R \geq 9.1$. For a discussion of the velocity profiles associated with these various solutions see Refs. 4 and 6. Recently, Brady and Acrivos⁸ have shown that the same similarity transformation applies for the flow in a channel or tube with an accelerating surface velocity, i.e., $u = Ex$, $v = 0$ at $y = h$, and found the solution structure for positive Reynolds number to be completely analogous to that described above.

This gap in the similarity solutions raises a question as to what happens to the flow in a very long porous tube as the suction velocity is increased from zero, and, more generally, a question as to what extent do *any* of the similarity solutions represent a realizable flow. Not knowing of the gap in the similarity solutions we would expect, for a porous tube of very long but finite length L , that as $h/L \rightarrow 0$ the similarity solution would become a better and better approximation to the actual flow over most of the region within the tube. The exception for a tube with suction is at the tube inlet, $x = L$ [a nondimensional region of $O(h/L)$], where the inlet velocity does not necessarily have the similarity form but rather is determined by conditions exterior to the tube. That is, we would expect the inlet velocity profile to *decay* into the fully developed, similarity form as $x \rightarrow 0$, provided the tube was of sufficient length.

In Sec. II we shall show that this is indeed the case for a tube with uniform suction provided $R \leq 2.3$, but that once R exceeds this critical value the flow within the entire tube is determined by the inlet condition and is not in general of the similarity form. In Sec. III we shall show that the same conclusions apply for the flow in a porous channel with uniform suction even though a similarity solution exists for all R . Here, the critical Reynolds number above which the flow can be said to be determined by the inlet conditions is approximately 6. Brady and Acrivos⁹ have shown that a very similar phenomenon occurs for the flow in a tube or channel with an accelerating surface velocity—that is, above a critical Reynolds number the structure of the flow is fundamentally different from the similarity form and is determined by, in this case, the end condition. There are, however, differences between these two situations, and we shall take up some of these in Sec. IV. The only other work that appears to have addressed this question of the decay of the inlet velocity profile into the similarity form is that of Raithby and Knudsen.¹⁰ These authors considered only porous channel flow for $R = 15$ and 30 and reached the same conclusion regarding the preservation of the inlet velocity profiles. They also reported some experimental results to confirm their numerical computations. Our results are in essential agreement with theirs, but we go further in showing the continuous evolution of the effect of the inlet condition with increasing Reynolds number, as well as presenting results for the porous tube problem. We shall only consider flows caused by suction ($R > 0$); those due to injection ($R < 0$) apparently (Ref. 10) agree well with the similarity solution as x now goes to $+\infty$.

II. FLOW IN A FINITE TUBE

To resolve the paradoxical situation of having no similarity solutions in the Reynolds number range $2.3 < R < 9.1$, we consider the flow in a very long, but finite, tube [there being no such thing as a truly infinite (or semiinfinite) tube]. Referring to Fig. 1 we denote the length of the tube by L and its radius by h , with $h/L \ll 1$ for very long tubes. The geometry and boundary condition at the tube wall lead to the natural scalings: the radial velocity, v , $O(V)$; the radial coordinate, r , $O(h)$; the axial coordinate, x , $O(L)$; and from continuity the axial velocity, u , $O[V(L/h)]$. The pressure p is scaled with the inertial terms as $O[\rho V^2(L/h)^2]$. With these scalings the nondimensional Navier–Stokes equations, equation of continuity for an incompressible fluid, and boundary conditions become, as $h/L \rightarrow 0$,

$$u \frac{\partial u}{\partial x} + v \frac{\partial u}{\partial r} + \frac{\partial p}{\partial x} = \frac{1}{R} \left\{ \frac{1}{r} \frac{\partial}{\partial r} r \frac{\partial u}{\partial r} + O\left[\left(\frac{h}{L}\right)^2\right] \right\}, \quad (1)$$

$$\frac{\partial p}{\partial r} = O\left[\left(\frac{h}{L}\right)^2\right], \quad (2)$$

$$\frac{\partial u}{\partial x} + \frac{1}{r} \frac{\partial}{\partial r} r v = 0, \quad (3)$$

and

$$u = 0, \quad v = 1, \quad \text{at } r = 1, \quad (4)$$

$$\frac{\partial u}{\partial r} = v = 0, \quad \text{at } r = 0. \quad (5)$$

Here $R \equiv \rho V h / \mu$ is the Reynolds number.

As $h/L \rightarrow 0$ Eqs. (1)–(3) are seen to be the axisymmetric form of the boundary-layer equations, with the exception that the transverse coordinate r is $O(1)$ and the Reynolds number appears as a parameter. Note further that neither R nor the equations contains L explicitly; thus as long as $h/L \ll 1$ the absolute scale of L is immaterial, i.e., the tube can be *arbitrarily* long. It is not difficult to see that the similarity solution satisfies (1)–(5) as well as the full equations of motion.

To complete the specifications for the boundary-layer equations, we need to impose an “initial” condition at the tube inlet $x = 1$, $u(1, r) = u_i(r)$. One possibility is that the inlet condition is just the similarity solution evaluated at $x = 1$, $u_i(r) = -f(r)/r$, but this is by no means the only possibility. It should be clear that Eqs. (1)–(3) do not apply within a nondimensional distance of $O(h/L)$ of the end, and rather than being of the similarity form the inlet velocity profile should be determined by the flow conditions exterior to the tube. For example, if we had a tube of nondimensional length 2 which was porous only over the first half, $0 < x < 1$, we would expect the inlet velocity to be a parabolic Poiseuille profile, which is not a similarity solution except for $R \equiv 0$.¹¹ The only requirement that must be satisfied by the inlet velocity profile is conservation of mass—as much fluid enters the tube as leaves through the porous walls. Integrating the equation of continuity over a cross section yields the following relation between volumetric flux and axial position:

$$\int_0^1 u(x,r)r dr = -x. \quad (6)$$

Thus, to determine the flow in an arbitrarily long porous tube and thereby investigate the applicability of the similarity solution, we need to solve Eqs. (1)–(5) for a given inlet velocity profile satisfying (6).

At first glance, it may appear that the similarity solution must hold as $x \rightarrow 0$ because all the fluid has been removed through the wall by $x = 0$, giving $u \rightarrow 0$ as $x \rightarrow 0$. However, Eqs. (1)–(3) are parabolic in x and having specified the inlet condition, it is improper to impose any condition at $x = 0$. From (6) we know that the volumetric flux through the tube is zero at $x = 0$, but this does not mean that u itself is zero. Just as Eqs. (1)–(3) are not valid within a region of $O(h/L)$ of the inlet, they are not necessarily valid within an $O(h/L)$ region near $x = 0$. As shown by Brady and Acrivos⁹ for the accelerating-wall tube flow, when u does not vanish as $x \rightarrow 0$ (dimensional x approaching zero on the length scale L) a proper rescaling of the equations of motion results in an inviscid region of flow near $x = 0$ with an effective Reynolds number $(L/h)R$. In this inviscid region the nonvanishing axial velocity “collides” with its mirror image from negative x (or with a wall at $x = 0$; the difference being unimportant because to a first approximation the flow is inviscid), is turned around, and flows back towards the inlet. Thus, the boundary-layer equations (1)–(3) must be viewed as applying in an “outer” region whose solution must match with the solution in the inviscid collision region as $x \rightarrow 0$.

Fortunately, a detailed solution in the collision region is not necessary,⁹ for matching alone serves to determine how the nonvanishing axial velocity is turned around. Matching requires that the vorticity divided by r be conserved along streamlines in the turning process, and since the volumetric flux must also be zero, together they require¹²

$$u_0(\eta) = -u_0(1 - \eta), \quad 0 \leq \eta \leq \frac{1}{2}, \quad \text{at } x = 0, \quad (7)$$

where $\eta = r^2$ and u_0 denotes the limiting form of the solution of (1)–(5) as $x \rightarrow 0$. Condition (7) simply states that for a solution of the boundary-layer equations in the porous tube to be consistent with the flow in the inviscid collision region the axial velocity profile must satisfy (7) at $x = 0$. Note also that the similarity solution gives $u_0 \equiv 0$ and satisfies (7).

In summary, our analysis of the equations of motion for the flow in a long porous tube has led to the following conclusions: The boundary-layer equations (1)–(3) apply over the entire length of the tube except at the inlet $x = 1$ and possibly at the origin $x = 0$. At the inlet there is a singular region of extent $O(h/L)$ within which the flow described by (1)–(3) matches with that outside the tube. As a first approximation in h/L this matching condition is simply that $u(1,r) = u_i(r)$, the inlet velocity profile. If the axial velocity found by solving (1)–(5) with a given $u_i(r)$ does not vanish as $x \rightarrow 0$, then there is a collision region at the origin whose structure is such that condition (7) must be satisfied. It is the realization that the boundary-layer equations describing the motion in a long porous tube are not valid near $x = 0$ and the inclusion of a collision region there that allows us to obtain solutions for all Reynolds numbers.

For a given $u_i(r)$ the flow in the tube is determined numerically in much the same way as was done in Ref. 9. The time-dependent term $\partial u / \partial t$ is added to the left-hand side of (1), and at a given time step the solution is found by marching in x from the inlet to the origin. If the axial velocity at $x = 0$ found by linear extrapolation from the two preceding grid points does not vanish, condition (7) is used. That is, the axial velocity for $0 \leq \eta \leq \frac{1}{2}$ is extrapolated to $x = 0$, and (7) determines the velocity profile for $\eta > \frac{1}{2}$, i.e., how the fluid turns around. A time step is taken and the marching procedure repeated, adjusting if necessary the velocity profile at $x = 0$. This entire sequence is continued until a steady state is obtained. A time-dependent or iterative scheme is needed when a collision region is present because the reverse flow near the origin influences the motion “upstream,” which in turn influences the velocity profile at $x = 0$ through Eq. (7). We chose a time-dependent scheme because it was simple to implement and follows closely the true dynamics of the process. The finite-difference scheme used space-centered differences in the r direction, first-order upwind differences in the x direction,¹³ and stepped forward in time explicitly in the x direction but implicitly in the r direction. The implicit formulation in r results in a tridiagonal system of equations at each axial position x which can be easily solved, thus enhancing the stability without loss in computational speed. Generally a mesh size of 26×26 was used; computations with finer or coarser meshes showed little variation. The unknown pressure gradient was found via (6) in the manner described in Ref. 9. The initial condition at $t = 0$ was either the $R \equiv 0$ solution, or the solution computed at a previous Reynolds number. Finally, a steady state was considered reached when the difference in the pressure gradient between time steps was less than 9×10^{-7} everywhere.

Two inlet velocity profiles were investigated; a parabolic Poiseuille profile, $u_i(r) = -4(1 - r^2)$, and a uniform profile, $u_i(r) = -2$ for all r . These two profiles represent in some sense the extremes between a very long tube with a nonporous section for $x > 1$ and a porous tube open to a large mass of fluid for which a uniform inlet profile seems reasonable. Other profiles may be used and will lead to similar re-

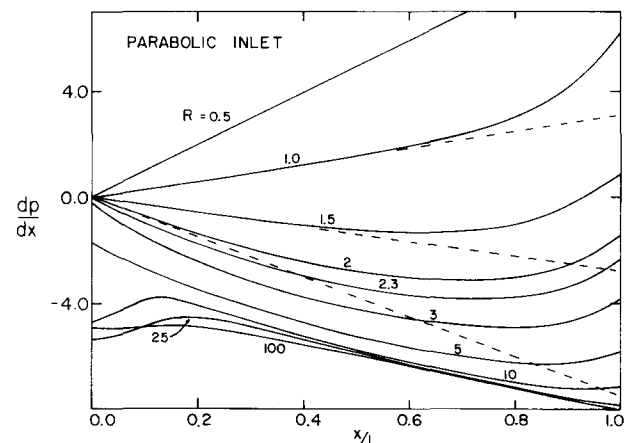


FIG. 3. The pressure-gradient profiles for the axisymmetric flow in a finite tube with a parabolic inlet velocity profile at $R = 0.5, 1, 1.5, 2, 2.3, 3, 5, 10, 25$, and 100 . The dashed lines correspond to the pressure-gradient profiles predicted by the similarity solution at $R = 1, 1.5$, and 2 .

sults, although profiles of extreme shape may exhibit temporal instability at large Reynolds numbers.

The results for the parabolic inlet profile are shown in Fig. 3 where the pressure gradient is plotted as a function of x for various values of the Reynolds number. The dashed lines are the pressure gradient computed from the similarity solution at $R = 0.5, 1.0, 1.5$, and 2.3 (the upper portion of the β/R vs R curve). The pressure gradient profiles show very clearly that the similarity solution accurately represents the flow in a porous tube over most of its length provided the Reynolds number is less than one (the same holds for the velocity profiles). As R increases, however, the flow predicted by the similarity solution and that in a finite tube agree over a smaller and smaller region near the origin, until at $R = 2.3$ the flows agree only at $x = 0$. Above this critical Reynolds number a collision region appears at the origin, and the flow in a finite tube has a structure fundamentally different from that of the similarity solution. We say fundamentally different because the mathematical form of the solution near $x = 0$ is not linear in x . The streamline pattern at $R = 10$ presented in Fig. 4 shows clearly the presence of reverse flow and a collision region at the origin. Flows for Reynolds numbers greater than 100 were not computed.

Pressure gradient profiles for the uniform inlet velocity profile are shown in Fig. 5. Again the dashed lines are from the similarity solution at $R = 1, 1.5, 2, 25$, and 100 . The similarity solutions for $R = 25$ and 100 are from the branch labeled A in Fig. 2 and correspond to a velocity profile which is uniform for all r except at the surface $r = 1$ where an $O(R^{-1})$ thick boundary layer develops to satisfy the no-slip condition. Apart from the rapid change in dp/dx near $x = 1$ resulting from the violation of the no-slip condition by the uniform inlet profile, we see the same general features as in the parabolic inlet case. The similarity solution is valid for small R , but once the critical Reynolds number 2.3 is reached a collision region develops at the origin. Unlike the parabolic inlet, however, when $R \geq 25$ the similarity solution and the actual flow start to agree again at the origin. This agreement grows in x until at $R = 100$ it is complete over the entire length of the tube except at the inlet, where the uniform inlet profile does not take into account the boundary layer at the wall. Had we modified the inlet profile to include a boundary layer, agreement would have been complete up to $x = 1$. Thus, at sufficiently large Reynolds number, given

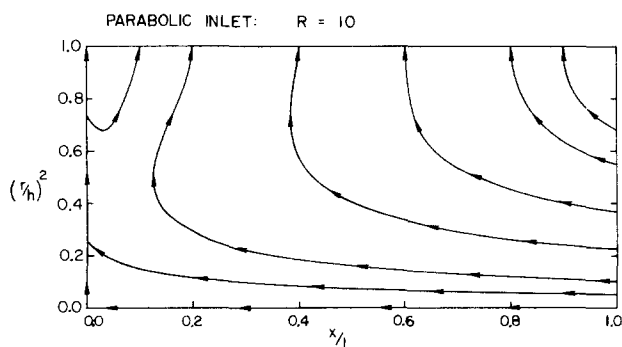


FIG. 4. The streamline pattern for the flow in a porous tube at $R = 10$ with a parabolic inlet profile. Note the presence of reverse flow and a collision region at $x = 0$.

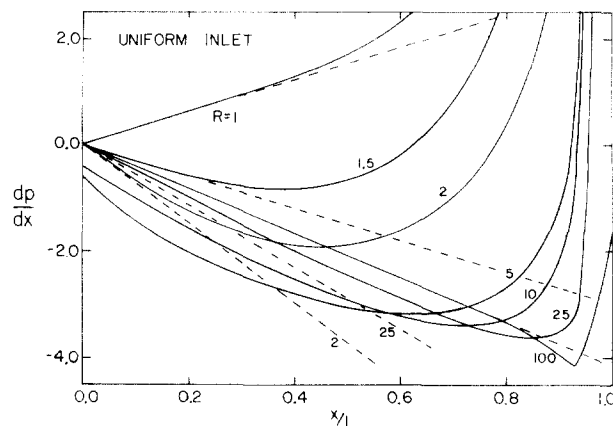


FIG. 5. The pressure-gradient profiles for the axisymmetric flow in a finite tube with a uniform inlet velocity profile at $R = 1, 1.5, 2, 5, 10, 25$, and 100 . The dashed lines correspond to the pressure-gradient profiles predicted by the similarity solution at $R = 1, 1.5, 2, 25$, and 100 . The lines for $R = 25$ and 100 come from the curve labeled A in Fig. 2.

an inlet profile which is of the similarity form, the similarity solution will be a valid approximation over most of the tube's length.

The conclusion to be drawn is that below the critical Reynolds number of 2.3 the flow in a finite tube asymptotically approaches the similarity solution as $x \rightarrow 0$ irrespective of the inlet profile (at least as far as the inlet profiles investigated in this work are concerned—it is not known whether other more “extreme” inlet profiles will result in a collision region at Reynolds numbers below 2.3). Above the critical Reynolds number however, the inlet profile influences the flow throughout the entire tube, resulting in a structure which is in general different from that predicted by the similarity solution. Only if the inlet condition is of the similarity form might the flow be described by this solution. A physical explanation of why the inlet profile does not necessarily decay into the fully developed, similarity form (when it exists) is easy to give. The deviation of the inlet profile from the similarity solution can be viewed as a disturbance or perturbation. This disturbance is convected along with the incoming fluid and is dampened by viscosity. As the Reynolds

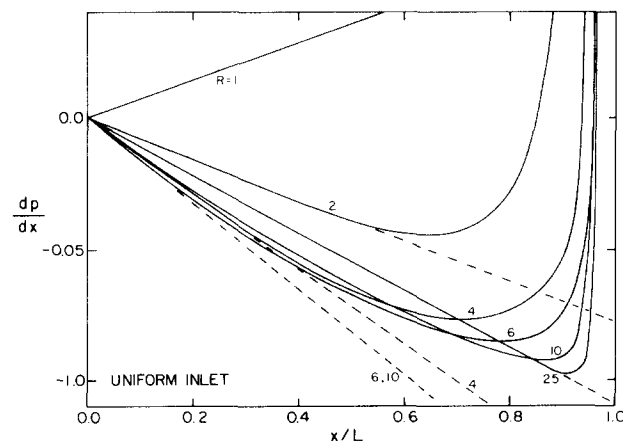


FIG. 6. The pressure-gradient profiles for the flow in a channel with a uniform inlet velocity profile at $R = 1, 2, 4, 6, 10$, and 25 . The dashed lines are the pressure-gradient profiles predicted by the similarity solution at $R = 2, 4, 6, 10$, and 25 ; the lines for $R = 6$ and 10 are indistinguishable.

number increases the action of viscosity decreases, and ultimately the convective motion carries the disturbance all the way to the origin. The inlet or end effect is then felt throughout the entire tube.

III. FLOW IN A FINITE CHANNEL

To investigate the validity of the similarity solutions for the flow in a uniformly porous channel the analysis of Sec. II was repeated for this geometry. Recall that for a porous channel there exists at least one similarity solution for all R . The results for the uniform inlet velocity profile are shown in Fig. 6 where a comparison is made between the pressure gradient in a finite channel and that predicted by the similarity solution. As in the porous tube case the effect of the inlet condition propagates inward with increasing Reynolds number until at $R \approx 6$ it appears to have reached the origin. However, unlike the porous tube flow, a collision region does *not* develop for larger R . Rather, the agreement between the two solutions starts increasing again because the uniform inlet is the similarity solution at large R . It seems that the "disturbance" due to the inlet profile not agreeing with the similarity solution for finite R is not quite strong enough for a collision region to form at the origin.

Pressure gradient profiles for the parabolic inlet profile presented in Fig. 7 also show that the inlet profile decays into the similarity solution for $R < \sim 6$.¹⁴ For $R > 6$ however, we have the rather surprising result that the pressure gradient appears to be approximately linear in x as $x \rightarrow 0$ but with a slope that does not correspond to any similarity solution. The same is true for the computed velocity profiles. Furthermore, no collision region forms at $x = 0$. Refining the mesh near $x = 0$ had no effect on the results, nor does increasing the Reynolds number up to as high as 200. Raithby and Knudson¹⁰ also computed velocity profiles which were apparently linear in x but not similarity solutions. This raises the question of how can there be solutions for the flow in a porous channel which appear to be of the similarity form— $u = x$ times a function of y —but not similarity solutions?

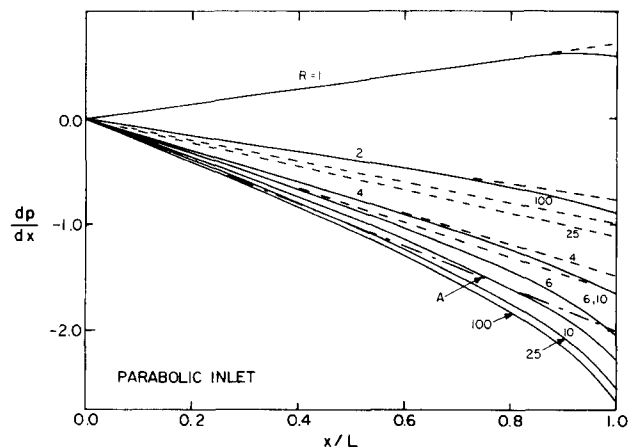


FIG. 7. The pressure-gradient profiles for the flow in a channel with a parabolic inlet velocity profile at $R = 1, 2, 4, 6, 10, 25$, and 100 . The dashed lines are the pressure-gradient profiles predicted by the similarity solution at $R = 1, 2, 4, 6, 10, 25$, and 100 . The broken line labeled A is the pressure gradient predicted by the stability analysis of Ref. 15.

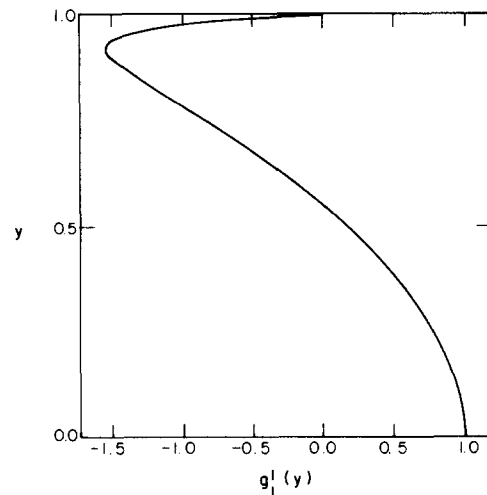


FIG. 8. The perturbation to the x component of velocity $g'_1(y)$ at $R = 36.4$ from the spatial stability analysis of Ref. 15.

The answer to this question can be found in the analysis of Durlafsky and Brady¹⁵ who considered the spatial stability of the similarity solutions to small perturbations of the form $x \lambda g'_n(y)$, much in the same way as is done for the Blasius solution for high-Reynolds-number flow over a flat plate. Solutions to the boundary-layer equations exist of the form

$$u = x f'(y) + \sum_{n=1}^{\infty} c_n x \lambda_n g'_n(y), \quad (8)$$

where $\{\lambda_n\}$ and $\{g'_n\}$ are eigenvalues and corresponding eigenfunctions. The solution to a given inlet condition will in general be a linear combination of the above form, provided the difference between the solution and the similarity solution is in some sense small, i.e., the amplitudes $\{c_n\}$ are small. Durlafsky and Brady¹⁵ have shown that the minimum eigenvalue λ_1 asymptotically approaches unity from above as $R \rightarrow \infty$ and attains this asymptotic value to within a few percent for Reynolds numbers as small as 20. Thus, at large Reynolds numbers the first eigensolution is approximately linear in x .

The first eigenfunction $g'_1(y)$ at a Reynolds number of 36.4 is shown in Fig. 8. At this Reynolds number λ_1 is 1.002. If this eigensolution is combined as in Eq. (8) with the similarity solution corresponding to a uniform inlet with an amplitude c_1 of $-\frac{1}{2}$, the resulting velocity profile is quite close to the parabolic inlet profile. Combining the perturbation to the pressure gradient associated with this eigensolution and amplitude with that of the similarity solution gives a "predicted" slope of approximately -2.02 for the parabolic inlet (asymptotically as $R \rightarrow \infty$ a predicted slope of -2). The straight line labeled A in Fig. 7 corresponds to this prediction and is seen to agree well with the actual pressure gradient for $x < 0.3$. The deviation of dp/dx from linearity near $x = 1$ is due to the presence of additional eigensolutions in, and the finite amplitude of, the perturbation caused by the parabolic inlet profile.

This stability analysis also allows us to explain why the pressure gradient in a porous tube with a parabolic inlet condition is almost linear at high Reynolds numbers but with an

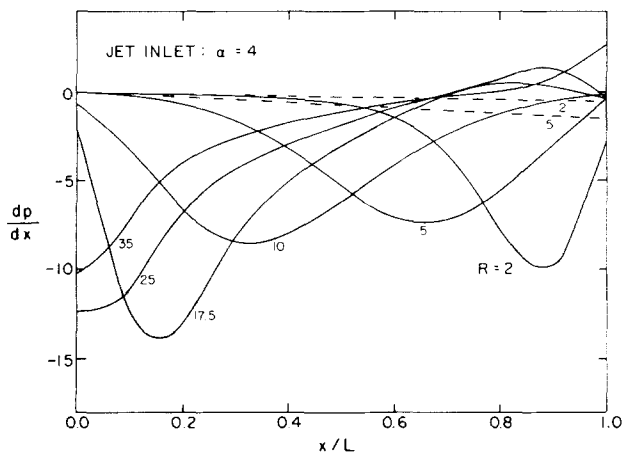


FIG. 9. The pressure-gradient profiles for the flow in a channel with a jet inlet condition with $\alpha = 4$ at $R = 2, 5, 10, 17.5, 25$, and 35 . The dashed lines are the pressure-gradient profiles predicted by the similarity solution at $R = 2$ and 5 .

intercept near -4 at $x = 0$ (cf. Fig. 3). As shown in Ref. 15, as $R \rightarrow \infty$ the first eigensolution has $\lambda_1 \rightarrow 0$ which, when combined with an amplitude of -2 with the similarity solution/uniform profile (the asymptotic, $R \rightarrow \infty$, form of the solution from the curve labeled A in Fig. 2), gives quite closely the parabolic inlet profile. With $\lambda = 0$ the perturbation to the pressure gradient is now a constant rather than proportional to x as with $\lambda = 1$, and with the amplitude -2 this constant is -4 .¹⁶ Thus, the stability analysis predicts that at high Reynolds numbers the flow in a porous tube with a parabolic inlet profile should have a pressure gradient which is linear in x with the slope of the similarity solution but offset by the constant amount -4 . As is evident in Fig. 3 this is very much the case for $R = 100$. [The discrepancy near $x = 0$ is due to the collision region through Eq. (7) not accounting for the boundary layer at $r = 1$.]

The parabolic inlet profile for the porous channel seems to be adequately represented by the eigensolution in Eq. (8) and can be considered a "small" perturbation. In order to investigate the behavior of larger perturbations and to see whether they can give rise to collision regions, inlet velocity profiles in the form of a jet concentrated on the centerline were tried. Using the classical profile for a two-dimensional jet¹⁷ modified to conserve mass, the inlet profiles were of the form

$$u_i(y) = -(\alpha/\tanh \alpha)(1 - \tanh^2 \alpha y),$$

where α is an adjustable constant which determines the strength of the jet. Here $\alpha \equiv 0$ reduces to the uniform inlet case. With this inlet condition, $\alpha = 2$ did not give rise to a collision region even for Reynolds numbers as large as 150. It should be added, however, that at these high Reynolds numbers neither the pressure gradient nor the velocity profile was linear in x . For $\alpha = 3$ a collision region first appeared around $R \approx 30$ and persisted for all larger R . For $\alpha = 4$, whose pressure gradient profiles are shown in Fig. 9, the collision region appeared at $R \approx 17$. It is not known, however, if there is a limiting minimum Reynolds number below which a collision region would not form regardless of how concentrated was the jet. Thus, it seems that the strength of

the perturbation for $\alpha > 2$ is sufficient to give rise to a collision region.

Even though the flow in a porous channel is somewhat different from that in a tube and does not necessarily have a collision region, the same conclusions can be drawn: Below a critical Reynolds number of approximately 6 the flow in a channel asymptotically approaches the similarity solution as $x \rightarrow 0$.¹⁸ Above this Reynolds number the inlet condition influences the flow throughout the entire channel.

IV. CONCLUSIONS

The results of the previous sections have shown that at large Reynolds numbers the flow everywhere in a finite, but arbitrarily long, uniformly porous channel or tube is influenced by the inlet condition. For the flow in a tube, once the critical Reynolds number of 2.3 is reached, the similarity solution loses validity as the effect of the inlet is felt throughout the entire tube and a collision region forms at the origin. At large Reynolds numbers ($R > 50$), the similarity solution may regain validity provided the inlet profile corresponds to a similarity solution. This should be viewed as an exception rather than the rule, for the inlet velocity profile is determined in large part by the region exterior to the tube and will not normally correspond to that of a similarity solution. For the flow in a finite channel, the conclusions are essentially the same—above a Reynolds number of approximately 6 the inlet condition influences the flow throughout the entire channel. Here, however, a collision region does not necessarily form at the origin, and only for inlet profiles which differ significantly from the similarity solution does a collision region appear.

In their study of the accelerating-wall problem Brady and Acrivos⁹ came to very much the same conclusions. The critical Reynolds number for the tube problem coincided precisely with the point where the similarity solutions cease to exist. At larger Reynolds numbers, however, they found no tendency for the flow to return to the form predicted by the similarity solution. There are two reasons for this difference. First, the maximum Reynolds number for which a flow was computed by Brady and Acrivos⁹ was 70, and the similarity solutions do not reappear until 147. Thus, there was no similarity solution to "return to." Second, and perhaps more importantly, the end conditions used in Ref. 9 differed significantly from the similarity form. For the accelerating-wall tube flow at large Reynolds number the strength of the return flow (equivalent to the inlet condition here) diminishes as $O(R^{-1/2})$. However, the end conditions used in Ref. 9 returned the fluid more or less as a concentrated jet along the centerline with a velocity of magnitude $O(1)$ rather than $O(R^{-1/2})$ —that is, a "large" perturbation from the similarity form. It is quite possible that if the end condition for the accelerating-wall tube flow corresponded more closely to the similarity solutions, the flow throughout the rest of the tube would also have agreed.

For the accelerating-wall channel flow Brady and Acrivos⁹ found that there existed a critical Reynolds number of 57 above which a collision region formed at the origin independent of the end conditions which they considered. In this

study whether a collision region forms or not depends on the inlet condition and the Reynolds number. Again, the probable explanation for the different behavior is that the two end conditions used in Ref. 9 were large perturbations from the similarity solution, but quite "similar" to each other. Although the porous and accelerating wall problems have some differences in detail, in both cases the same important conclusion is reached: as the Reynolds number increases above a certain value, the end condition influences the flow throughout the entire channel or tube.

Only the limited class of inlet velocity profiles which are monotonic was investigated. Other profiles may be used (and may be appropriate for a particular problem), but they should not lead to any fundamentally different results. Also, in most experimentally realizable porous channel or tube flows, the normal velocity is proportional to the pressure difference across the porous boundary; since the pressure varies with axial position so too would the suction velocity. Only when the pressure drop across the wall is large compared with that along the tube will the wall be *uniformly* porous. Our analysis is thus, strictly speaking, limited to this case. It is a straightforward matter, however, to modify the procedure in Sec. II to handle a variable, pressure-dependent, suction velocity.

Finally, the method used here of allowing for a collision region as a matching condition and for assessing the validity of similarity solutions has found application in other problems. In particular, it has been shown that the similarity solution for the flow between two rotating disks loses validity in much the same way as the porous channel flow.¹⁹ These results together with those of Brady and Acrivos⁹ and many others are a strong indication that similarity solutions should be viewed with caution, as they may have only a limited range of validity.

ACKNOWLEDGMENTS

The help of L. Durlofsky in preparing Figs. 2 and 8 and for many discussions is greatly appreciated, as is A. M. Thuer's contribution to the numerical programming.

This research was supported in part by a DuPont Young Faculty Grant.

¹A. S. Berman, J. Appl. Phys. **24**, 1232 (1953).

²R. M. Terrill, Aeronaut. **15**, 297 (1964).

³R. M. Terrill, Aeronaut. **16**, 323 (1965).

⁴R. M. Terrill and P. W. Thomas, Appl. Sci. Res. **21**, 37 (1969).

⁵W. A. Robinson, J. Eng. Math. **10**, 23 (1976).

⁶F. M. Skalak and C-Y. Wang, Appl. Sci. Res. **33**, 269 (1977).

⁷Terrill and Thomas (Ref. 4) reported two solutions for $R < 0$, but as shown by Durlofsky and Brady (Ref. 15) only one is a legitimate, porous tube, solution.

⁸J. F. Brady and A. Acrivos, J. Fluid Mech. **112**, 127 (1981).

⁹J. F. Brady and A. Acrivos, J. Fluid Mech. **115**, 427 (1982).

¹⁰G. D. Raithby and D. C. Knudsen, J. Appl. Mech. **41**, 896 (1974).

¹¹To be formally correct, we require the solution in the region $0 < x < 1$ to match as $x \rightarrow 1$ from below with the solution in an "inner region" of extent $O(h/L)$ centered about $x = 1$. In turn we require the solution in the region $1 < x < 2$, the parabolic profile, to match as $x \rightarrow 1$ from above with the solution in the inner region. In the limit $h/L \rightarrow 0$ this inner transition region becomes the line $x = 1$, and as a first approximation we set the inlet profile equal to the parabolic profile at $x = 1$.

¹²Analysis of the matching requirement with the collision region does not yield a unique solution. There are many ways in which to conserve both the vorticity divided by r along streamlines and mass in an inviscid flow, each leading to a condition very much like (7). Our choice for (7) represents the "most reasonable" one. For a further discussion of this point see Ref. 9.

¹³Space-centered differences were also used in the x direction and gave results essentially identical with those obtained by upwind differencing. However, the space-centered method tended to exhibit spatial and temporal wiggles near the inlet $x = 1$ because of the sudden change in boundary condition which occurs there; the wiggles being most pronounced for the uniform inlet profile and at large R . This is just a manifestation of the invalidity of the boundary-layer equations in the singular region near $x = 1$; a region we did not attempt nor wish to resolve.

¹⁴It is difficult to determine accurately the Reynolds number at which the end effect first reaches the origin. We can say, however, that it occurs between $R = 5$ and $R = 7$.

¹⁵L. Durlofsky and J. F. Brady, Phys. Fluids **27**, 1068 (1984).

¹⁶In fact, $\lambda = 0$ is not just a perturbation but an eigensolution—it satisfies the full Navier-Stokes equations with arbitrary amplitude. For a further discussion of this point see Ref. 15.

¹⁷H. Schlichting, *Boundary-Layer Theory* (McGraw-Hill, New York, 1968), 6th ed., p. 173.

¹⁸Even with $\alpha = 4$, the solution is linear for small x at $R = 5$, but as seen in Fig. 9 soon loses this linearity with increasing R .

¹⁹J. F. Brady, J. Fluid Mech. (to be submitted).